JOURNAL OF SOLID STATE CHEMISTRY 74, 260–267 (1988)

The Polyphosphides $NbMn_2P_{12}$, $MoMn_2P_{12}$, and WMn_2P_{12} with $TiMn_2P_{12}$-Type Structure

U. D. SCHOLZ, W. JEITSCHKO,* AND M. REEHUIS

Anorganisch-Chemisches Institut, Universität Münster, Wilhelm-Klemm-Strasse 8, D-4400 Münster, West Germany

Received October 3, 1987

The title compounds are new and were prepared by reaction of the elemental components in a tin flux. They crystallize with the monoclinic ($C2/c$) $TiMn_2P_{12}$-type structure, which was refined for $NbMn_2P_{12}$ (R = 0.044 for 70 variable parameters and 1688 structure factors) and $MoMn_2P_{12}$ (R = 0.020 for 70 variables and 2871 F values). Chemical bonding in these compounds can be rationalized on the basis of classical two-electron bonds. In this simple bonding model the Mn atoms with octahedral P coordination ("d^2sp^3 hybrid") obtain a ("low spin") d^5 system. They are displaced from the centers of their P octahedra to permit Mn–Mn bonding (Mn–Mn distances of 285.1 and 287.7 pm for the Nb and Mo compounds, respectively), thus compensating their spins. The early transition-metal atoms have square-antiprismatic P coordination ("d^4sp^3 hybrid"). In this model their fifth d orbital is filled with one (Nb) or two (Mo, W) electrons. Consequently $MoMn_2P_{12}$ and WMn_2P_{12} are diamagnetic, while $NbMn_2P_{12}$ shows paramagnetism with a magnetic moment of $\mu = 1.96\ \mu_B$. The metallic conductivity of the three compounds is rationalized by the overlap of bonding and antibonding bands ("semimetal"). None of the compounds TMn_2P_{12} (T = Ti, Nb, Mo, W) becomes superconducting down to 1.8 K. © 1988 Academic Press, Inc.

Introduction

The classical model of the two-electron bond is useful in organic as well as in solid-state chemistry. In solids, formed between highly electropositive metals and the main-group elements, it allows us to predict the near-neighbor coordinations within the polyanion ("Zintl compounds"). It has been applied successfully also to rationalize and predict the electrical conductivity behavior (*1–3*) and the atomic environments (*4*) of essentially covalent solids with low coordination numbers (tetrahedral, square-planar, and octahedral) composed of the main group elements and the late and post-transition metals. The two-electron bond model was used recently also to rationalize the structures and physical properties of $MoFe_2P_{12}$, WFe_2P_{12} (*5*), and $TiMn_2P_{12}$ (*6*), where the early transition-metal atoms have square-antiprismatic coordination of eight phosphorus atoms. Here we show the usefulness of the two-electron bond model to rationalize the magnetic properties of new compounds with $TiMn_2P_{12}$-type structure.

Synthesis and Chemical Properties

The compounds were prepared by reaction of the elemental components in a tin

* To whom correspondence should be addressed.

0022-4596/88 $3.00

Copyright © 1988 by Academic Press, Inc.
All rights of reproduction in any form reserved.

flux. Starting materials were powders of niobium (<250 μm, 99.8%), molybdenum (<150 μm, 99.95%), tungsten (<150 μm, 99.98%), manganese (<40 μm, 99.9%), and pieces of red phosphorus (Hoechst–Knapsack: "ultrapure") and tin (99.9%). They were mixed in various atomic ratios as, for example, Nb : Mn : P : Sn = 5 : 2 : 10 : 17, Mo : Mn : P : Sn = 1 : 2 : 30 : 20, W : Mn : P : Sn = 1 : 2 : 15 : 20 and sealed in evacuated silica tubes. The samples were annealed for up to 2 weeks at various temperatures of between 600 and 950°C and usually quenched to room temperature. The tin-rich matrix was dissolved in slightly diluted (1 : 1) hydrochloric acid, which practically does not attack the transition-metal polyphosphides. Various amounts of the binary polyphosphides NbP_2 (*7, 8*), MoP_2, α-, β-WP_2 (*7–10*), and the three stacking variants of MnP_4 (*11–15*) were frequently observed in the reaction products. They were mechanically separated from the crystals of the ternary compounds under the microscope. Energy dispersive fluorescence analyses in a scanning electron microscope did not reveal impurity elements heavier than sodium, like silicon or tin (detectability limits 0.5%).

The crystals of the new compounds were well developed with diameters of up to 100 μm and no preferred growth directions. They are stable in air and not attacked by nonoxidizing acids or bases. $NbMn_2P_{12}$ dissolves within a few hours in concentrated nitric acid, while $MoMn_2P_{12}$ and WMn_2P_{12} were only weakly attacked under these conditions. Under prolongated treatment with aqua regia crystals of $MoMn_2P_{12}$ and WMn_2P_{12} showed rounded-off edges and corners.

Physical Properties

The crystals are brittle and black with metallic luster. The electrical conductivities of these three polyphosphides were measured with a two-probe device for cold-pressed pellets squeezed between tungsten blocks. The conductivities were determined repeatedly both on heating and cooling at constant current, measuring the voltage differences with a compensator. Within the range of liquid nitrogen temperature and 250°C the conductivities of the three compounds decreased on heating by between a factor of 3.5 for $MoMn_2P_{12}$ and 4.5 for $NbMn_2P_{12}$. The absolute values of the specific resistivities were about 0.02 Ω cm for $NbMn_2P_{12}$ and 0.04 Ω cm for $MoMn_2P_{12}$ and WMn_2P_{12}. Considering the uncertainties in the estimates for the contacting areas and the porosities of the pellets, these values were judged to be correct within factors of about 3. Thus, both the temperature dependencies and the absolute values of the electrical conductivities are typical for metallic conductors.

Samples of TMn_2P_{12} (T = Ti, Nb, Mo, W) were investigated for superconductivity using the *ac* susceptibility method. None of these metallic polyphosphides showed a transition to a superconducting state down to 1.8 K.

The magnetic susceptibilities of the three polyphosphides were determined with a Faraday balance (*16, 17*) for polycrystalline samples of crystals selected under a microscope with total weights of 35, 6, and 2 mg for $NbMn_2P_{12}$, $MoMn_2P_{12}$, and WMn_2P_{12}, respectively. $MoMn_2P_{12}$ and WMn_2P_{12} are both weakly diamagnetic; however, because of the small sample weights these values could not be determined accurately.

In contrast, $NbMn_2P_{12}$ is strongly paramagnetic with a room temperature susceptibility of $\chi = 1.59(\pm 0.03) \times 10^{-3}$ cm^3/formula unit. Its temperature dependence follows the Curie–Weiss law. After correction for the temperature-independent part of the susceptibility a paramagnetic Curie temperature of $\theta = +2(\pm 1)$ K and an effective magnetic moment of $\mu_{exp} = 1.96(\pm 0.02)\ \mu_B$ was obtained from the slope

of the $1/\chi$ vs T plot (Fig. 1). This value compares rather well with the theoretical (spin only) value for one unpaired electron of $\mu_{eff} = 1.73\ \mu_B$, considering that the experimental values are usually somewhat higher for the transition elements of the second (Nb) and third long period, due to spin-orbit coupling. The correction for the temperature-independent part of the susceptibility of $\chi = -86 \times 10^{-6}$ cm^3/formula unit—obtained from the deviation from the straight line of the $1/\chi$ vs T plot—is small, however, of the expected magnitude if we consider that the diamagnetism is superimposed by the Pauli paramagnetism.

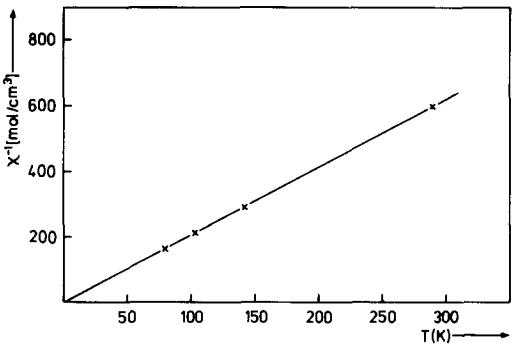

FIG. 1. Reciprocal magnetic susceptibility of $NbMn_2P_{12}$ as a function of temperature.

Structure Refinements

Single crystals of $NbMn_2P_{12}$ and $MoMn_2P_{12}$ were investigated in precession cameras with Mo$K\alpha$ radiation. They showed the Laue symmetry $2/m$ and the systematic extinctions (reflections hkl were observed only for $h + k = 2n$; $h0l$ only for $l = 2n$) led to the space groups Cc and $C2/c$ of which the centrosymmetric group $C2/c$ was found to be correct during the structure refinements. This is also the space group of $TiMn_2P_{12}$ and the structure refinements showed $NbMn_2P_{12}$ and $MoMn_2P_{12}$ to be completely isotypic with $TiMn_2P_{12}$. No superstructure reflections corresponding to the primitive monoclinic cell of $NbFe_2P_{12}$ (*18*) were observed.

The lattice constants (Table I) were obtained by least-squares fits of the Guinier powder data, recorded at 24°C, using α-quartz ($a = 491.30$ pm, $c = 540.46$ pm) as a standard. To assure proper assignment of indices to the numerous diffraction lines, the observed patterns were carefully compared with the patterns calculated (*19*) from the refined structures of $NbMn_2P_{12}$ and $MoMn_2P_{12}$, respectively. As an example the evaluation of the powder pattern of WMn_2P_{12} is shown in Table II.

Intensity data for the structure refinements were recorded in an automated four-circle diffractometer with graphite-monochromated Mo$K\alpha$ radiation, a scintillation counter, and a pulse-height discriminator. The background was determined at both ends of each $\theta/2\theta$ scan. All reflections

TABLE I

LATTICE CONSTANTS AND CALCULATED DENSITIES OF POLYPHOSPHIDES WITH $TiMn_2P_{12}$ STRUCTURE[a]

	a (pm)	b (pm)	c (pm)	β (°)	V (nm^3)	ρ_c(g/cm^3)
$TiMn_2P_{12}$[b]	1605.8(3)	579.4(1)	1063.6(2)	115.23(1)	0.8952	3.928
$NbMn_2P_{12}$	1609.8(2)	578.1(1)	1065.2(1)	115.63(1)	0.8937	4.280
$MoMn_2P_{12}$	1597.2(2)	571.8(1)	1054.6(1)	115.86(1)	0.8667	4.437
WMn_2P_{12}	1597.6(2)	571.7(1)	1053.7(1)	115.85(1)	0.8662	5.102

[a] Standard deviations in the last listed digits are given in parentheses.
[b] Data from Ref. (*6*).

TABLE II

POWDER PATTERN OF WMn_2P_{12} WITH $TiMn_2P_{12}$-TYPE STRUCTURE[a]

hkl	Q_o	Q_c	I_o	I_c	*hkl*	Q_o	Q_c	I_o	I_c
200	192	194	w	34	−423	2231	2231	vw	6
110	351	354	vw	4	313	2319	2318	vw	10
−202	382	382	m	58	−713	2335	2334	w	24
−111	402	402	w	28	421	2365	2365	vw	15
002	443	445	vw	6	114	2389	2390	vw	11
111	529	530	vs	100	−802	2518	2518	vw	11
−311	660	661	m	37	512	2600	2600	vw	16
−112	673	671	vw	8	−224	2685	2685	w	19
−402	706	707	w	26	−621	—	2693	—	7
310	741	741	w	19	−515	2697	2696	w	28
400	773	774	vw	14	−115	2815	2815	vw	16
−312	803	802	vw	5	−623		2815		16
202	895	894	m	52	−804	2831	2828	vw	6
112	929	927	vw	6	602	2951	2954	vw	8
311	1045	1045	vw	12	422		2954		2
−113	1165	1163	m	40	620	2966	2965	w	18
−313	1167	1166	m	47	131	2978	2977	vw	14
020	1225	1224	w	32	024	3002	3003	vw	6
−511	1307	1307	s	71	−132	3118	3119	vw	13
−512	1320	1321	vw	8	330	3187	3189	s	63
021	1336	1335	vw	4	−624	3209	3209	m	32
−221	1400	1401	m	38	−715	—	3218	—	10
−602	1418	1419	vw	10	711	3233	3236	s	57
−204	1460	1461	w	17	−406	3240	3242	w	27
510	1515	1515	vw	11	−606	—	3442	—	5
−404	1531	1530	w	25	115	3454	3454	vw	31
113	1547	1547	w	28	331	—	3492	—	5
−513	1559	1557	w	33	−913	3500	3498	vw	10
312	1571	1570	m	37	−425		3499		9
−222	1607	1606	w	22	−225	3558	3558	w	26
022	1671	1669	w	25	404	—	3577	—	11
402	1732	1731	vw	5	−914	3698	3701	vw	16
600	1742	1742	w	30	−822	3736	3741	vw	9
−314	1756	1753	vw	7	−531	3753	3754	vw	7
004	1781	1779	w	18	−911	3766	3760	vw	14
−421	1855	1853	vw	16	−532	—	3768	—	7
−604	1985	1986	w	19	−821	3920	3919	vw	12
420	2000	1998	vw	9	332	4018	4018	vw	7
−223	2035	2034	vw	8	−806	4029	4029	vw	6
222	2118	2118	m	35	−824	4050	4052	vw	4
−712	2225	2226	vw	4					

[a] All observed reflections and all those with calculated intensities $I_c > 4$ are listed. $Q = 100/d^2$ (nm^{-2}); vw, very weak; w, weak; m, medium; s, strong; vs, very strong. The intensities were calculated assuming positional parameters as obtained in the structure refinement of $MoMn_2P_{12}$.

within one half of the reciprocal sphere up to $2\theta = 90°$ were measured. This resulted in a total of 7697 reflections for the crystal of $NbMn_2P_{12}$ (with dimensions of $20 \times 60 \times 60$ μm^3) and 7430 reflections for the $MoMn_2P_{12}$ crystal ($70 \times 70 \times 130$ μm^3). Empirical absorption corrections were made from ψ-scan data. The linear absorption coefficients $\mu(MoK\alpha)$ are 59.6 and 63.0 cm^{-1} for the Nb and Mo compound, respectively. After omitting reflections with $F_o < 3\sigma(F_o)$ and averaging equivalent values (internal residual $R_i = 0.042$), 1688 structure factors remained for the refinement of the structure of $NbMn_2P_{12}$ (for $MoMn_2P_{12}$: $R_i = 0.018$ for 2871 averaged nonequivalent reflections).

As starting parameters for the full-matrix least-squares refinements we used the positional parameters as obtained for $TiMn_2P_{12}$ (*6*). The atomic scattering factors (*20*) were corrected for anomalous dispersion (*21*). The weighting schemes were according to the counting statistics, and parameters accounting for isotropic secondary extinction were refined and applied to the calculated structure factors. For structure refinements with isotropic thermal parameters (a total of 32 variables) conventional residuals of $R = 0.047$ and $R = 0.022$ were obtained for $NbMn_2P_{12}$ and $MoMn_2P_{12}$, respectively. Structure refinements with ellipsoidal thermal parameters reflected (as is frequently observed) the inadequacy of the absorption corrections from ψ-scan data. Least-squares calculations with variable occupancy parameters showed no significant deviations from full occupancies for any atomic position. The extrema varied for $NbMn_2P_{12}$ from 98.6(6)% occupancy for the P(3) position to 101.6(5)% for the P(5). For the more accurately determined structure of $MoMn_2P_{12}$ the occupancy parameters were even closer to the ideal values: 99.8(2)% for the P(5) and P(6) positions and 100.2(1)% for the Mo position (standard deviations in the position of the least-significant digit are given in parentheses). In the final least-squares cycles the occupancy parameters were again kept at the ideal values. The conventional residuals and the weighted residuals were $R = 0.044$ and $R_w = 0.050$ for $NbMn_2P_{12}$ (70 variable parameters, 1688 structure factors) and $R = 0.020$, $R_w = 0.017$ for $MoMn_2P_{12}$ (70 variables, 2871 F's). The atomic parameters and interatomic distances are given in Ta-

TABLE III

POSITIONAL AND THERMAL PARAMETERS OF $NbFe_2P_{12}$ AND $MoFe_2P_{12}$[a]

Atom	C2/c	x	y	z	B_{equiv}
Nb	4e	0	0.3034(1)	¼	0.167(7)
Mn	8f	0.18181(4)	0.1902(1)	0.04609(7)	0.206(8)
P(1)	8f	0.15561(8)	0.1757(3)	0.2432(1)	0.31(2)
P(2)	8f	0.46770(9)	0.4520(3)	0.0732(1)	0.27(2)
P(3)	8f	0.38340(9)	0.0526(3)	0.4952(1)	0.29(2)
P(4)	8f	0.32246(8)	0.3268(2)	0.1656(1)	0.27(2)
P(5)	8f	0.43754(9)	0.1465(2)	0.3346(1)	0.31(2)
P(6)	8f	0.27326(8)	0.3208(3)	0.4250(1)	0.28(2)
Mo	4e	0	0.30466(3)	¼	0.227(2)
Mn	8f	0.18005(1)	0.19185(4)	0.04611(2)	0.234(3)
P(1)	8f	0.15185(2)	0.17637(7)	0.24114(4)	0.346(5)
P(2)	8f	0.46747(3)	0.45695(7)	0.07447(4)	0.361(6)
P(3)	8f	0.38405(3)	0.05383(7)	0.49650(4)	0.365(5)
P(4)	8f	0.32252(2)	0.32453(7)	0.16561(4)	0.322(5)
P(5)	8f	0.43898(2)	0.14087(7)	0.33388(4)	0.353(6)
P(6)	8f	0.27252(2)	0.32251(7)	0.42396(4)	0.333(5)

[a] Standard deviations in the place of the last listed position are given in parentheses. The last column lists the equivalent isotropic thermal parameters B_{equiv} (×100 in units of nm^2).

bles III and IV. Listings of observed and calculated structure factors can be obtained from the authors (*22*). A stereoplot and a projection of the $TiMn_2P_{12}$-type structure are shown in Figs. 2 and 3.

Discussion

In the polyphosphides of the transition metals with high phosphorus content the metal atoms usually have octahedral phosphorus coordination. Square-planar (Ni, Pd), tetrahedral (Cu, Ag), and linear twofold coordination (Au) are also known (*23*). The polyphosphides with $TiMn_2P_{12}$-type structure are the first examples, where the (early) transition-metal atoms have eight phosphorus neighbors forming an almost regular square-antiprism. The manganese atoms have octahedral phosphorus coordination and the phosphorus atoms are all tetrahedrally coordinated either to two metal and two phosphorus atoms or to one metal and three phosphorus atoms.

Using the classical two-electron bond model and oxidation numbers (where the

TABLE IV

INTERATOMIC DISTANCES (pm) IN $NbMn_2P_{12}$ AND $MoMn_2P_{12}$[a]

	$NbMn_2P_{12}$			$MoMn_2P_{12}$	
Nb:	P(5)	255.8(2×)	Mo:	P(5)	248.6(2×)
	P(1)	264.2(2×)		P(1)	257.4(2×)
	P(2)	266.3(2×)		P(2)	261.0(2×)
	P(3)	267.9(2×)		P(3)	262.9(2×)
Mn:	P(4)	220.8	Mn:	P(4)	220.0
	P(4)	222.8		P(4)	221.7
	P(6)	223.3		P(6)	221.9
	P(3)	229.9		P(3)	226.6
	P(1)	231.5		P(1)	229.1
	P(2)	233.2		P(2)	229.8
	Mn	285.1		Mn	287.7
P(1):	P(4)	220.0	P(1):	P(4)	219.8
	P(6)	220.6		P(6)	221.1
	Mn	231.5		Mn	229.1
	Nb	264.2		Mo	257.4
P(2):	P(5)	226.1	P(2):	P(5)	227.5
	P(2)	228.6		P(2)	228.3
	Mn	233.2		Mn	229.8
	Nb	266.3		Mo	261.0
P(3):	P(6)	222.7	P(3):	P(6)	222.0
	P(5)	229.5		P(5)	229.6
	Mn	229.9		Mn	226.6
	Nb	267.9		Mo	262.9
P(4):	P(1)	220.0	P(4):	P(1)	219.8
	P(5)	220.8		P(5)	219.8
	Mn	220.8		Mn	220.0
	Mn	222.8		Mn	221.7
P(5):	P(4)	220.8	P(5):	P(4)	219.8
	P(2)	226.1		P(2)	227.5
	P(3)	229.5		P(3)	229.6
	Nb	255.8		Mo	248.6
P(6):	P(6)	219.4	P(6):	P(6)	218.7
	P(1)	220.6		P(1)	221.1
	P(3)	222.7		P(3)	222.0
	Mn	223.3		Mn	221.9

[a] All metal–metal and metal–phosphorus distances less than 360 pm are listed. The shortest nonbonding phosphorus–phosphorus distance is a P(3)–P(5) distance of 289.8 pm in both structures. Standard deviations computed from those of the lattice constants and the positional parameters are all equal or less than 0.3 pm in $NbMn_2P_{12}$ and 0.1 pm in $MoMn_2P_{12}$.

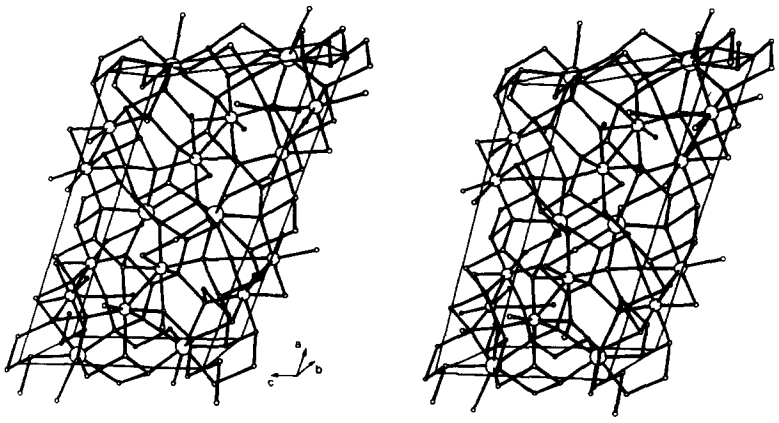

FIG. 2. Stereoplot of the structures of $TiMn_2P_{12}$, $NbMn_2P_{12}$, and $MoMn_2P_{12}$. The differences in the positional parameters of the three refinements of this structure are too small to be discernible on the scale of this plot. The early transition metals, the manganese, and the phosphorus atoms are drawn with large, medium, and small circles, respectively.

two electrons of the transition metal–phosphorus bonds are *counted* as belonging to the phosphorus atoms) the eight phosphorus atoms per formula unit with two metal and two phosphorus neighbors obtain oxidation number -1, and the remaining phosphorus atoms with one metal and three phosphorus neighbors obtain oxidation number zero. This is in agreement with the phosphorus atoms obtaining an electron octet ("sp^3 hybrid").

The manganese atoms have octahedral phosphorus coordination. The MnP_6 octahedra form pairs with one common edge, and the manganese atoms are slightly displaced from the centers of their octahedra to form a manganese–manganese bond. This is almost the same bonding situation as for the manganese atoms in the three modifications of MnP_4 (*11–15*). There the bonding was rationalized with oxidation numbers according to $Mn^{+2}(P_4)^{-2}$, i.e., the manganese atoms obtain a d^5 system. For the bonds to the six phosphorus neighbors the manganese atoms need six orbitals ("d^2sp^3 hybrid") to interact with the $3s$ and $3p$ orbitals of the phosphorus atoms. The corresponding 12 bonding electrons we have already counted at the phosphorus atoms. The five electrons of the manganese atoms, which do not participate in the manganese–phosphorus bonds, can be accommodated in the three $\sim t_{2g}$ orbitals. Two of these we assume to be doubly occupied with a total of four electrons and the third one can overlap with the corresponding orbital of the neighboring manganese atom to split into a bonding and an antibonding ("molecular") orbital. The bonding orbital is filled with two electrons, one from each manganese atom, while the antibonding orbital remains empty in this idealized description. Thus we have accommodated all valence electrons of the manganese atoms with compensated spins and we expect this part of the structure to be essentially diamagnetic as is indeed observed for the three modifications of MnP_4, which, in addition, are also semiconductors (*11, 14, 15*).

Having assigned oxidation numbers to the manganese and phosphorus atoms the balance has to be made up by the early transition metals (T). We thus obtain the general formula $T^{+4}(Mn^{+2})_2(P^0)_4(P^{-1})_8$, i.e., the titanium atoms obtain a d^0 system, the niobium atoms a d^1 system, and the molybde-

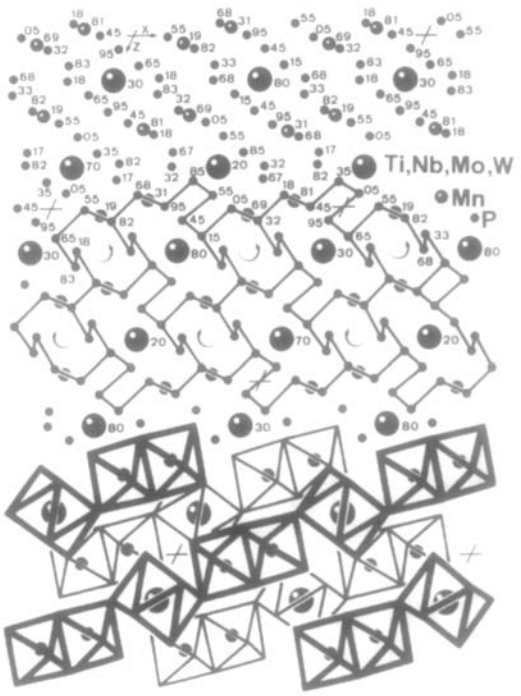

FIG. 3. Projection of the monoclinic $TiMn_2P_{12}$-type structure along the twofold axis. In the upper part of the drawing the heights of the atoms are indicated in hundredths of the projection direction. Below that the P–P bonds within the three-dimensional network of the phosphorus-poly-"anion" are shown. The 18-membered P-rings surrounding the early transition-metal atoms in this projection are connected by chains of P atoms, which spiral clock- and anticlockwise along the projection direction. In the lower part of the figure the linkages of the coordination polyhedra of the metal atoms are shown. The MnP_6 octahedra form pairs with a common edge. All other linkages of the MnP_6 octahedra and the quadratic antiprisms TP_8 (T = Ti, Nb, Mo, W) are via corners.

num and tungsten atoms a d^2 system. For the eight bonds of each T atom to its square-antiprismatic phosphorus coordination we need eight orbitals ("d^4sp^3 hybrid"), which overlap with the valence orbitals of the phosphorus atoms to form an empty antibonding band and a bonding band which is filled by the electrons we have counted already at the phosphorus atoms. In this simple bonding description the remaining d_{z^2} orbital of the T atom is unoccupied (Ti), singly occupied (Nb), or doubly occupied (Mo, W). We thus expect diamagnetism for $TiMn_2P_{12}$, $MoMn_2P_{12}$, and WMn_2P_{12} and paramagnetism for $NbMn_2P_{12}$ as is indeed observed.

This simple bonding description had allowed us to correctly predict the magnetic properties of the $TiMn_2P_{12}$-type compounds before we actually determined them. Nevertheless this description could certainly be improved by band structure calculations. For instance, the Mn–Mn bond distances of around 285 pm are rather long. Shorter Mn–Mn distances, however, are not possible because this would cause even greater deviations from the ideally tetrahedral Mn–P–Mn (109°) and octahedral P–Mn–P (90°) angles (Table V). Such geometrically required deviations from the ideal bond distances and angles do not need to be energetically strictly unfavorable. We can assume that at least some interactions, which with ideal bond angles are negligible, gain in energy with increasing distortions, as it was shown for the structurally related compounds TX_2 with marcasite or arsenopyrite structure (*24*). Nevertheless, the simplicity of the two-electron bond model makes it attractive also for the rationalization of those structures (*11, 25*).

At first sight the metallic conductivity of the $TiMn_2P_{12}$-type compounds is unex-

TABLE V

COMPARISON OF THE BOND DISTANCES AND BOND ANGLES AROUND THE MANGANESE–MANGANESE BOND IN $TiMn_2P_{12}$-TYPE COMPOUNDS[a]

	$TiMn_2P_{12}$	$NbMn_2P_{12}$	$MoMn_2P_{12}$
Mn–P(4)	283.5	285.1	287.7
Mn–P	220.9	220.8	220.0
Mn–P(4)	223.1	222.8	221.7
P(4)–Mn–P	79.38	79.97	81.28
P–Mn–P	100.62	100.03	98.72

[a] The Mn–Mn bond is centrosymmetric. Standard deviations of the distances (pm) and angles (°) are all equal or less than 0.2 pm and 0.04°.

pected. However, the band gaps are already small for the late transition-metal polyphosphides (*26*). For polyphosphides, containing the early transition metals with higher coordination numbers, broader bands can be expected, and once the band gap is closed ("semimetal"), the temperature dependence of the conductivity inverses, and the compound becomes a metallic conductor. Slight overlaps of bands which are labeled "bonding" and "antibonding" in the simple two-electron bond picture may well be responsible for the decreasing bond strength of the Mn–Mn bond in going from $TiMn_2P_{12}$ to $MoMn_2P_{12}$ (Table V).

Acknowledgments

We are indebted to Dr. M. H. Möller for the collection of the single-crystal X-ray data. Dipl.-Chem. L. Boonk and Mr. K. Wagner are thanked for the tests for superconductivity and for the work on the scanning electron microscope. We also acknowledge Dr. G. Höfer (Heraeus Quarzschmelze) and the Hoechst AG for generous gifts of silica tubes and ultrapure red phosphorus. This work was supported by the Deutsche Forschungsgemeinschaft and the Fonds der Chemischen Industrie.

References

1. H. Krebs and W. Schottky, "Halbleiterprobleme," Vol. 1, Vieweg & Sons, Brunswick (1954).
2. E. Mooser and W. B. Pearson, *in* "Progress in Semiconductors" (A. F. Gibson, R. E. Burgess, and F. A. Kröger, Eds.), p. 104, Wiley, New York (1960).
3. F. Hulliger, *Struct. Bonding* **4,** 83 (1968).
4. E. Parthé, *Acta Crystallogr. Sect. B* **29,** 2808 (1973).
5. U. Flörke and W. Jeitschko, *Inorg. Chem.* **22,** 1736 (1983).
6. U. D. Scholz and W. Jeitschko, *Z. Anorg. Allg. Chem.* **540/541,** 234 (1986).
7. F. Hulliger, *Nature (London)* **204,** 775 (1964).
8. S. Rundqvist, *Nature (London)* **211,** 847 (1966).
9. S. Rundqvist and T. Lundström, *Acta Chem. Scand.* **17,** 37 (1963).
10. R. Rühl and W. Jeitschko, *Monatsh. Chem.* **114,** 817 (1983).
11. W. Jeitschko and P. C. Donohue, *Acta Crystallogr. Sect. B* **31,** 574 (1975).
12. D. J. Braun and W. Jeitschko, *Z. Anorg. Allg. Chem.* **445,** 157 (1978).
13. B. I. Noläng and L.-E. Tergenius, *Acta Chem. Scand. A* **34,** 311 (1980).
14. W. Jeitschko, R. Rühl, U. Krieger, and C. Heiden, *Mater. Res. Bull.* **15,** 1755 (1980).
15. R. Rühl and W. Jeitschko, *Acta Crystallogr. Sect. B* **37,** 39 (1981).
16. R. Hempelmann, Dissertation, Universität Münster (1980).
17. W. Jeitschko and M. Reehuis, *J. Phys. Chem. Solids* **48,** 667 (1987).
18. U. D. Scholz and W. Jeitschko, to be published.
19. K. Yvon, W. Jeitschko, and E. Parthé, *J. Appl. Crystallogr.* **10,** 73 (1977).
20. D. T. Cromer and J. B. Mann, *Acta Crystallogr. Sect. A* **24,** 321 (1968).
21. D. T. Cromer and D. Liberman, *J. Chem. Phys.* **53,** 1891 (1970).
22. U. D. Scholz, Dissertation, Universität Dortmund (1985).
23. W. Jeitschko, U. Flörke, M. H. Möller, and R. Rühl, *Ann. Chim. (Paris)* **7,** 525 (1982).
24. S. D. Wijeyesekera and R. Hoffmann, *Inorg. Chem.* **22,** 3287 (1983).
25. W. Jeitschko, U. Flörke, and U. D. Scholz, *J. Solid State Chem.* **52,** 320 (1984).
26. U. Flörke and W. Jeitschko, *J. Less-Com. Metals* **86,** 247 (1982).